

Validation of Rainfall Data Observed by Using Disdrometer under Wet-Bulb Temperature Conditions

By H. J. Kim *et al.*

Reply to the referees' comments

In the following, the comments made by the referees appear in black, while our replies are in red, and the proposed modified text in the typescript is in blue.

Referee #1 comments

1. The authors have improved the manuscript by addressing the core concerns raised in the previous review round. But there are still some aspects that need improvement before it can be acceptable.

We appreciate your thorough review, which has contributed to improving the quality of our manuscript. We have systematically addressed all referees' comments to further strengthen the paper.

2. Introduction: There are numerous factors that influence precipitation, which the author categorizes into climatological, geographical, or topographical factors. However, most studies examine precipitation variations from the perspectives of thermodynamics and dynamics. It is recommended that the author reorganizes this parts.

We appreciate your detailed feedback. In response to the referee's suggestions, we have revised and expanded the section on precipitation analysis to provide a clearer explanation of the research background and objectives. The original text referenced dynamics and thermodynamics; we have further supplemented this content to clarify the research objectives.

🔗 Page 2, line 44-51

“Environmental factors that influence precipitation development exert both hydrodynamic effects, including variations in lower-level vertical flow and atmospheric convergence or divergence, and thermodynamic effects, such as increased atmospheric instability resulting from water vapor inflow and differences in vertical temperature distribution. The differences in the development of precipitation due to environmental influences from the perspectives of atmospheric dynamics and thermodynamics ultimately lead to variations in the total precipitation observed at the surface. Therefore, it is crucial to acquire data that accurately reflects the microphysical characteristics of precipitation to enhance precipitation monitoring. Furthermore, analyses based on long-term observational data are essential to identify the universal characteristics that account for the temporal variability of precipitation.”

3. Methods: There are too many mathematic equations in this manuscript. Please ensure that every symbol and operation is appropriately defined, such as the Gamma function, Γ , atan, the corresponding meanings should be explained.

The equations presented in the manuscript are essential for deriving the drop size distribution, rain rate, and wet-bulb temperature. We have carefully reviewed each symbol and operation. To facilitate comprehension of these equations, we provide the following explanations.

The gamma model, recognized for its reliability in representing DSD characteristics, was selected for analysis. The gamma model is a widely used DSD model that enables the derivation of rainfall characteristics by capturing both the flatness and the overall shape of the number concentration distribution. This model (Eq. (9)) is characterized by the shape parameter μ (Eq. (10)), slope parameter Λ (mm^{-1}) (Eq. (11)), and intercept parameter N_0 ($\text{mm}^{-1-\mu}\text{m}^{-3}$) (Eq. (12)).

The term “atan” in Eq. (15) denotes the inverse tangent function.

4. Results: For the comparative of hourly rainfall measurements obtained from 2DVD and rain gauge, such as results in Figures 5 and 6, it better to give the statistical significance of the regression equation, and provide more convincing results.

We appreciate your detailed and constructive review. To clarify the statistical significance of the rainfall data, we have included both the correlation coefficient and p-value in Figures 5 and 6. The results under all conditions indicate a statistically significant correlation.

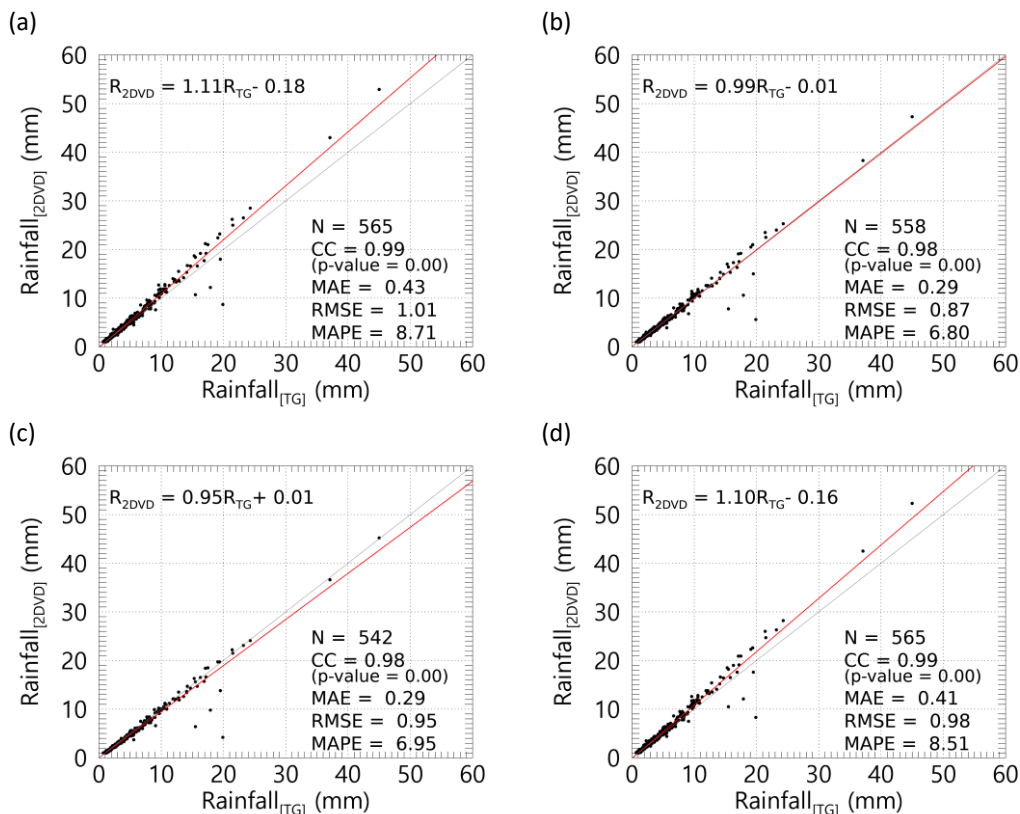


Figure 5: Comparison of rainfall observed using the tipping-bucket rain gauge and 2DVD when $T_w \geq 5$ °C ((a) Unfiltered, (b) Method 1, (c) Method 2, (d) Method 3). R_{2DVD} and R_{TG} denote the rainfall obtained from the 2DVD and a tipping-bucket rain gauge, respectively.

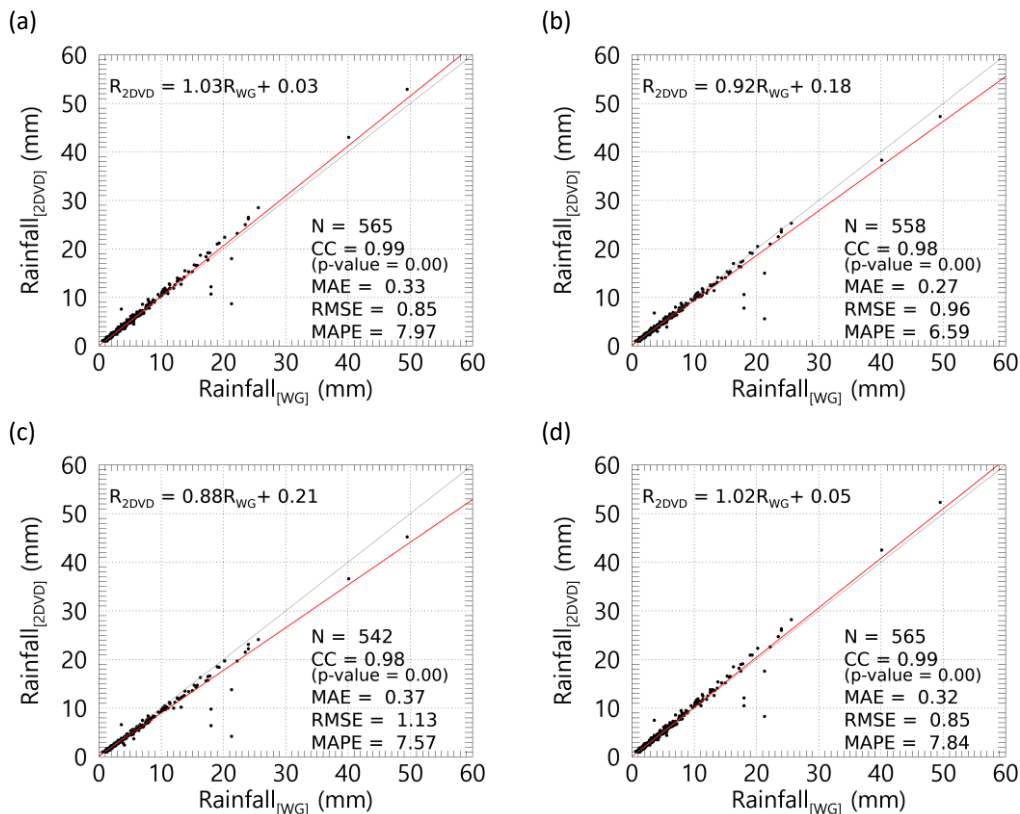


Figure 6: Comparison of rainfall observed using the weighing rain gauge and 2DVD when $T_w \geq 5 \text{ }^\circ\text{C}$ ((a) Unfiltered, (b) Method 1, (c) Method 2, (d) Method 3). R_{WG} denotes the rainfall obtained from a weighing rain gauge.

5. Conclusions: The conclusion section involved to many numeric expressions. It should concisely summarize the key findings and avoid restating detailed results. Instead, synthesize the main findings and propose possible directions for future research.

We appreciate the feedback provided and have revised the conventions accordingly. The primary numerical results are now presented without redundancy, and the main research findings are summarised concisely. Furthermore, we have included information on future research directions.

This study employed data collected from a 2DVD disdrometer in conjunction with traditional rain gauges to assess the precipitation measurements derived from the disdrometer under T_w conditions and to evaluate the reliability of the DSD model. Precipitation estimates derived from the quality control (QC) techniques implemented in this study exhibited a correlation coefficient of 0.98 or higher and an error rate of approximately 8.5% compared to precipitation measured by rain gauges under conditions where T_w was above $5 \text{ }^\circ\text{C}$. Additionally, the QC-processed precipitation data mitigated the overestimation present when QC methods were not applied to the disdrometer data. These findings indicate that QC methods demonstrated high reliability under rainfall conditions.

When both T_{air} and T_w were below $1 \text{ }^\circ\text{C}$, the fall velocity of precipitation particles decreased significantly,

with most velocities ranging from 0.5 to 3 m s⁻¹. This reduction results from a higher proportion of snow particles, which have a lower density than raindrops. These results are consistent with Ding et al. (2014), who reported that the proportion of raindrops decreases to less than 30% at temperatures below this threshold. When T_{air} ranged from 1 to 3 °C, the distribution of fall velocities was broader compared to cases where T_w was within the same interval, and deviations from the terminal velocity of raindrops were more pronounced. Therefore, hydrometeor classification during the QC process of disdrometer data should employ T_w as the primary environmental parameter for fall velocity analysis. This approach reduces errors in particle removal related to fall velocity distribution and improves the reliability of long-term rainfall measurements. As T_w decreased below 2 °C, quantitative precipitation errors increased because the filter ratio for particles of 3 mm or less rose to 30% or higher. In this temperature range, the likely coexistence of raindrops and solid particles reduces the reliability of conventional rainfall quality control methods. When snow particles are assumed to have melted, the correlation coefficient approached 0.9 even within the 0 to 1 °C range, and error variability decreased. These findings indicate that precipitation calculation reliability can be maintained under mixed-phase conditions (0 to 2 °C) if an appropriate snow particle density is applied. Verification of precipitation using a weighing rain gauge is recommended when T_w falls below 2 °C.

For DSD characteristics, the DSD shape remained consistent across different quality control methods at T_w above 2 °C. Below 2 °C, Method 1 ($\pm 40\%$ terminal velocity criterion) resulted in a higher number concentration of drops larger than 2 mm. In contrast, below 1 °C, Method 3 (Raupach et al., 2015) produced a pronounced, irregular distribution of number concentrations for diameters of 1 to 2 mm. These distortions in DSD shape, which depend on the quality control method, raise concerns regarding the reliability of derived DSD parameters. Consequently, only disdrometer data collected at T_w above 2 °C should be used to calculate DSD parameters and DSD-based rain rates.

Ensuring the reliability of dual-polarimetric radar-based quantitative precipitation estimation (QPE) parameterized by DSD characteristics is essential, given that DSD characteristics derived from disdrometer data vary with temperature. These temperature-dependent variations in DSD directly influence dual-polarimetric parameters and are likely to affect the QPE relationships used in radar-based precipitation estimation. Therefore, further research is required to investigate the impact of disdrometer data quality on QPE accuracy under different temperature conditions.

Referee #2 comments

1. It is recommended to change the way Tables A1-A4 are presented, as these tables currently fail to directly reveal the main information.

We appreciate your thoughtful review. In response to your feedback, we have revised the content to enhance its readability. Tables are organized by verification index to enable direct comparison of temperature and quality control (QC) methods.

🔗 Page 30-36, line 489-507

Table A1: a_1 of precipitation intensity derived from tipping-bucket rain gauge and 2DVD observations for each T_w range.

a_1	T1	T2	T3	T4	T5	T6	T7	T8	T9	T10
Unfiltered	5.88	3.74	3.72	4.40	2.11	0.73	1.46	1.05	1.09	1.06
Method 1	0.39	0.28	0.51	1.18	0.49	0.71	1.23	1.00	1.04	1.01
Method 2	0.70	0.58	0.37	0.59	0.34	0.87	1.03	0.98	1.00	0.96
Method 3	1.29	2.22	2.30	2.18	0.92	0.76	1.28	1.05	1.09	1.06
Method 1 (melted)	0.81	0.71	0.81	1.29	0.59	0.67	1.26	1.03	1.06	1.02
Method 2 (melted)	0.71	0.59	0.60	0.86	0.42	0.68	1.08	0.99	1.02	0.98
Method 3 (melted)	1.54	2.33	2.41	2.25	0.99	0.77	1.29	1.05	1.09	1.06

Table A2: a_0 of precipitation intensity derived from tipping-bucket rain gauge and 2DVD observations for each T_w range.

a_0	T1	T2	T3	T4	T5	T6	T7	T8	T9	T10
Unfiltered	0.12	0.11	0.25	0.11	0.32	0.43	0.01	0.04	0.04	0.06
Method 1	0.04	0.02	0.05	0.06	0.14	0.07	0.01	0.04	0.04	0.05
Method 2	0.01	0.00	0.01	0.03	0.08	0.02	0.00	0.03	0.04	0.06
Method 3	0.09	0.09	0.12	0.13	0.18	0.24	0.00	0.04	0.04	0.06
Method 1 (melted)	0.07	0.03	0.08	0.07	0.15	0.16	0.01	0.04	0.03	0.05
Method 2 (melted)	0.02	0.02	0.06	0.06	0.10	0.10	0.00	0.03	0.04	0.05
Method 3 (melted)	0.10	0.08	0.14	0.13	0.19	0.26	0.00	0.04	0.04	0.06

Table A3: RMSE of precipitation intensity derived from tipping-bucket rain gauge and 2DVD observations for each T_w range.

RMSE	T1	T2	T3	T4	T5	T6	T7	T8	T9	T10
Unfiltered	1.01	0.91	0.92	0.96	0.85	0.92	0.46	0.10	0.17	0.23
Method 1	0.17	0.18	0.12	0.21	0.29	0.20	0.30	0.09	0.12	0.16
Method 2	0.03	0.03	0.06	0.13	0.20	0.09	0.12	0.08	0.08	0.13
Method 3	0.24	0.44	0.47	0.49	0.33	0.43	0.25	0.10	0.17	0.23
Method 1 (melted)	0.16	0.10	0.15	0.25	0.28	0.31	0.32	0.09	0.13	0.16
Method 2 (melted)	0.09	0.14	0.15	0.17	0.25	0.21	0.14	0.08	0.09	0.13
Method 3 (melted)	0.27	0.46	0.51	0.51	0.35	0.46	0.26	0.10	0.17	0.23

Table A4: MAE of precipitation intensity derived from tipping-bucket rain gauge and 2DVD observations for each T_w range.

MAE	T1	T2	T3	T4	T5	T6	T7	T8	T9	T10
Unfiltered	0.44	0.47	0.56	0.45	0.45	0.40	0.16	0.06	0.10	0.16
Method 1	0.08	0.07	0.05	0.11	0.15	0.11	0.10	0.06	0.07	0.12
Method 2	0.01	0.01	0.04	0.07	0.10	0.06	0.05	0.05	0.05	0.09
Method 3	0.11	0.26	0.28	0.26	0.18	0.23	0.10	0.06	0.10	0.16
Method 1 (melted)	0.06	0.05	0.09	0.12	0.16	0.16	0.11	0.06	0.08	0.12
Method 2 (melted)	0.05	0.07	0.08	0.09	0.13	0.12	0.06	0.05	0.05	0.10
Method 3 (melted)	0.13	0.27	0.30	0.28	0.20	0.25	0.11	0.06	0.10	0.16

Table A5: MAPE of precipitation intensity derived from tipping-bucket rain gauge and 2DVD observations for each T_w range.

MAPE	T1	T2	T3	T4	T5	T6	T7	T8	T9	T10
Unfiltered	48.71	55.32	60.15	50.58	50.86	43.25	34.45	15.68	13.54	21.14
Method 1	28.57	56.67	27.24	34.01	37.07	56.39	31.27	17.96	12.04	16.83
Method 2	5.56	11.11	23.81	57.78	41.67	26.56	26.79	12.78	10.54	13.44
Method 3	38.75	49.04	51.11	47.07	45.58	46.25	25.58	15.68	13.54	21.14
Method 1 (melted)	26.33	21.39	34.06	31.87	42.73	38.50	31.64	18.03	12.37	16.51
Method 2 (melted)	17.78	23.33	27.88	31.87	45.37	44.88	27.62	12.84	11.00	15.80
Method 3 (melted)	40.50	49.24	50.27	47.38	46.46	45.30	28.44	15.68	13.54	21.14

Table A6: CC of precipitation intensity derived from tipping-bucket rain gauge and 2DVD observations for each T_w range.

CC	T1	T2	T3	T4	T5	T6	T7	T8	T9	T10
Unfiltered	0.97	0.97	0.93	0.95	0.74	0.23	0.85	0.99	0.99	0.99
Method 1	0.45	0.75	0.78	0.79	0.55	0.66	0.89	0.99	1.00	0.99
Method 2	0.98	0.94	0.60	0.67	0.57	0.91	0.97	0.99	1.00	1.00
Method 3	0.76	0.99	0.94	0.87	0.73	0.47	0.94	0.99	0.99	0.99
Method 1 (melted)	0.76	0.97	0.85	0.82	0.66	0.51	0.88	0.99	1.00	0.99
Method 2 (melted)	0.93	0.98	0.84	0.79	0.67	0.65	0.96	0.99	1.00	1.00
Method 3 (melted)	0.79	0.99	0.93	0.87	0.74	0.45	0.93	0.99	0.99	0.99

Table A7: a_1 of precipitation intensity derived from weighing rain gauge and 2DVD observations for each T_w range.

a_1	T1	T2	T3	T4	T5	T6	T7	T8	T9	T10
-------	----	----	----	----	----	----	----	----	----	-----

Unfiltered	7.36	3.39	3.98	3.86	2.25	2.15	1.37	1.01	1.03	1.03
Method 1	0.61	0.26	0.48	0.93	0.48	0.61	1.11	0.97	0.98	0.98
Method 2	0.53	0.58	0.21	0.46	0.28	0.80	0.88	0.95	0.94	0.93
Method 3	1.91	2.01	2.33	2.02	0.92	1.04	1.12	1.01	1.03	1.03
Method 1 (melted)	1.16	0.65	0.89	1.12	0.57	0.79	1.15	0.99	0.99	0.98
Method 2 (melted)	0.91	0.53	0.65	0.74	0.38	0.61	0.93	0.96	0.95	0.95
Method 3 (melted)	2.24	2.10	2.47	2.08	0.99	1.14	1.13	1.01	1.03	1.03

Table A8: a_0 of precipitation intensity derived from weighing rain gauge and 2DVD observations for each T_w range.

a_0	T1	T2	T3	T4	T5	T6	T7	T8	T9	T10
Unfiltered	0.09	0.12	0.27	0.09	0.24	0.06	0.04	0.04	0.02	0.01
Method 1	0.02	0.03	0.06	0.05	0.09	0.05	0.04	0.05	0.02	0.01
Method 2	0.01	0.00	0.01	0.03	0.06	0.01	0.05	0.03	0.03	0.02
Method 3	0.07	0.10	0.15	0.10	0.15	0.10	0.05	0.04	0.02	0.01
Method 1 (melted)	0.05	0.03	0.09	0.06	0.12	0.06	0.04	0.04	0.02	0.01
Method 2 (melted)	0.01	0.02	0.07	0.05	0.09	0.04	0.05	0.04	0.02	0.01
Method 3 (melted)	0.07	0.10	0.16	0.11	0.16	0.10	0.05	0.04	0.02	0.01

Table A9: RMSE of precipitation intensity derived from weighing rain gauge and 2DVD observations for each T_w range.

RMSE	T1	T2	T3	T4	T5	T6	T7	T8	T9	T10
Unfiltered	1.04	0.88	0.95	0.93	0.76	0.64	0.33	0.14	0.12	0.17
Method 1	0.13	0.17	0.13	0.19	0.28	0.20	0.20	0.13	0.10	0.14
Method 2	0.07	0.03	0.09	0.18	0.31	0.10	0.11	0.12	0.11	0.17
Method 3	0.22	0.41	0.52	0.45	0.29	0.21	0.16	0.14	0.12	0.17
Method 1 (melted)	0.11	0.13	0.16	0.23	0.26	0.16	0.21	0.13	0.10	0.13

Method 2 (melted)	0.04	0.18	0.14	0.17	0.29	0.18	0.09	0.12	0.11	0.15
Method 3 (melted)	0.27	0.44	0.55	0.48	0.30	0.22	0.16	0.14	0.12	0.17

Table A10: MAE of precipitation intensity derived from weighing rain gauge and 2DVD observations for each T_w range.

MAE	T1	T2	T3	T4	T5	T6	T7	T8	T9	T10
Unfiltered	0.44	0.46	0.57	0.43	0.43	0.31	0.15	0.08	0.07	0.12
Method 1	0.06	0.07	0.07	0.12	0.13	0.11	0.10	0.08	0.07	0.10
Method 2	0.02	0.01	0.06	0.11	0.15	0.07	0.07	0.07	0.07	0.12
Method 3	0.12	0.25	0.29	0.24	0.16	0.13	0.09	0.08	0.07	0.12
Method 1 (melted)	0.06	0.08	0.10	0.11	0.15	0.10	0.09	0.08	0.06	0.10
Method 2 (melted)	0.01	0.10	0.09	0.11	0.14	0.10	0.06	0.07	0.07	0.11
Method 3 (melted)	0.14	0.26	0.32	0.25	0.17	0.14	0.09	0.08	0.07	0.12

Table A11: MAPE of precipitation intensity derived from weighing rain gauge and 2DVD observations for each T_w range.

MAPE	T1	T2	T3	T4	T5	T6	T7	T8	T9	T10
Unfiltered	49.76	55.42	60.80	48.81	53.44	41.61	41.39	22.03	13.07	19.05
Method 1	25.71	63.33	41.35	41.49	36.12	79.17	38.21	22.17	14.21	21.89
Method 2	22.22	11.11	28.57	85.56	55.43	27.34	35.56	18.32	14.12	20.69
Method 3	42.13	49.58	52.32	44.83	46.50	37.92	34.21	22.03	13.07	19.05
Method 1 (melted)	30.25	31.05	36.50	29.44	49.92	32.10	37.80	22.22	13.91	21.50
Method 2 (melted)	8.89	35.56	34.62	42.75	58.79	40.35	34.42	17.78	14.24	22.16
Method 3 (melted)	43.48	49.81	51.47	45.14	46.83	38.15	37.14	22.03	13.07	19.05

Table A12: CC of precipitation intensity derived from weighing rain gauge and 2DVD observations for each T_w range.

CC	T1	T2	T3	T4	T5	T6	T7	T8	T9	T10
Unfiltered	0.98	0.97	0.90	0.93	0.88	0.89	0.95	0.98	0.99	0.99
Method 1	0.70	0.65	0.73	0.80	0.79	0.71	0.96	0.98	0.99	1.00
Method 2	0.82	0.94	0.45	0.75	0.78	0.92	0.98	0.98	1.00	1.00
Method 3	0.91	0.98	0.86	0.90	0.80	0.90	0.98	0.98	0.99	0.99
Method 1 (melted)	0.90	0.97	0.82	0.82	0.77	0.89	0.96	0.98	1.00	1.00
Method 2 (melted)	0.98	0.98	0.79	0.82	0.77	0.87	0.99	0.98	1.00	1.00
Method 3 (melted)	0.93	0.98	0.86	0.89	0.82	0.92	0.98	0.98	0.99	0.99

Table A13: Diameter channel information of the PARSIVEL disdrometer.

Channel number	Mid-value of channel (mm)	Diameter spread (mm)	Channel number	Mid-value of channel (mm)	Diameter spread (mm)
1	0.062	0.125	17	3.250	0.500
2	0.187	0.125	18	3.750	0.500
3	0.312	0.125	19	4.250	0.500
4	0.437	0.125	20	4.750	0.500
5	0.562	0.125	21	5.500	1.000
6	0.687	0.125	22	6.500	1.000
7	0.812	0.125	23	7.500	1.000
8	0.937	0.125	24	8.500	1.000
9	1.062	0.125	25	9.500	1.000
10	1.187	0.125	26	11.000	2.000
11	1.375	0.250	27	13.000	2.000
12	1.625	0.250	28	15.000	2.000
13	1.875	0.250	29	17.000	2.000
14	2.125	0.250	30	19.000	2.000
15	2.375	0.250	31	21.500	3.000
16	2.750	0.500	32	24.500	3.000

Table A14: Velocity channel information of the PARSIVEL disdrometer.

Channel number	Mid-value of channel (mm)	Velocity spread (mm)	Channel number	Mid-value of channel (mm)	Velocity spread (mm)
1	0.050	0.100	17	2.600	0.400
2	0.150	0.100	18	3.000	0.400
3	0.250	0.100	19	3.400	0.400
4	0.350	0.100	20	3.800	0.400
5	0.450	0.100	21	4.400	0.800
6	0.550	0.100	22	5.200	0.800
7	0.650	0.100	23	6.000	0.800
8	0.750	0.100	24	6.800	0.800
9	0.850	0.100	25	7.600	0.800
10	0.950	0.100	26	8.800	1.600

11	1.100	0.200
12	1.300	0.200
13	1.500	0.200
14	1.700	0.200
15	1.900	0.200
16	2.200	0.400

27	10.400	1.600
28	12.000	1.600
29	13.600	1.600
30	15.200	1.600
31	17.600	3.200
32	20.800	3.200